

F6-87-NC
Palygorskite

#10

SCALE - 1:250,000

DREDGE D8

2600-2100M

84ut transit
on 1/3.54 Hz



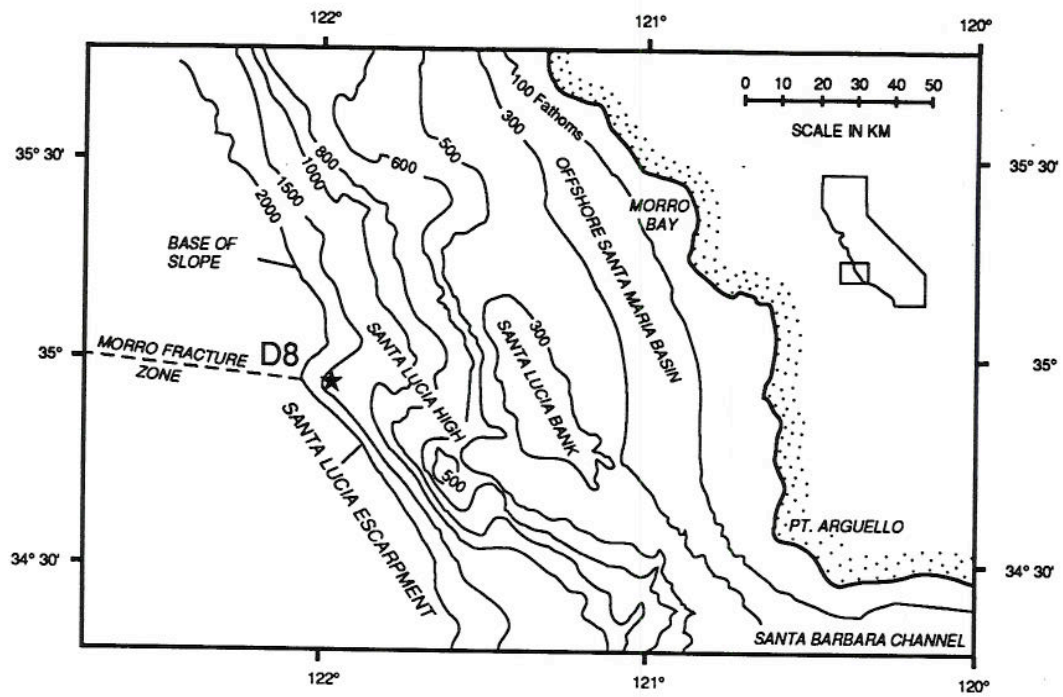


Figure 1 Gibbs et al.

anomaly at the fault to support
 ment. Acoustic basement offsets
 document vertical displacement.
 ide of the offshore Santa Maria
 d by the Hosgrl fault, which is
 workers. to have experienced
 ht-lateral slip (Graham and
 Hall et al., 1978; Silver,
 rance with this Neogene tectonic
 Culloch (1987) proposed formation
 Santa Maria Basin by
 His mapping shows that structures
 are en echelon, doubly
 with intervening lows, consistent
 sed basin development by
 nching. During the Pliocene
 ocene, the offshore Santa Maria
 affected by a component of plate
 approximately normal to the
 gin. In particular, Crouch et al.
 and seismic reflection data showing
 d verging thrust faults along the
 of the basin, and McCulloch
 and seismic profiles showing
 d compressional deformation in
 d seaward parts of the basin.
 some of the post-Miocene fold axes
 lts across the continental margin.

Acquisition and Processing

define deep structure and determine
 ip with the shallow features across
 e acquisition of RU-3 was designed
 ration and crustal scale imaging,
 lowing excellent resolution in the
 n. The energy source consisted of
 tuned, air gun array fired at 50-m
 180 channel, digital streamer was
 hydrophone section length of 25 m,
 e offset of 1700 m. Data were
 s at a sample interval of 4 ms.
 s at the processing started with summation of
 in shot gathers to increase
 ratio and reduce data volume.
 owed by sorting to nominal 45-fold
 nt gathers and by velocity analysis
 ervals. Short-period multiple and
 suppression was accomplished using
 convolution (32-ms gap, 200-ms
), and water bottom-multiple
 enhanced by frequency-wave number
 lled to the common midpoint gathers.
 migrated after stack using a 45°
 nce algorithm. The display
 consisted of time-variant, band-pass
 automatic in control.

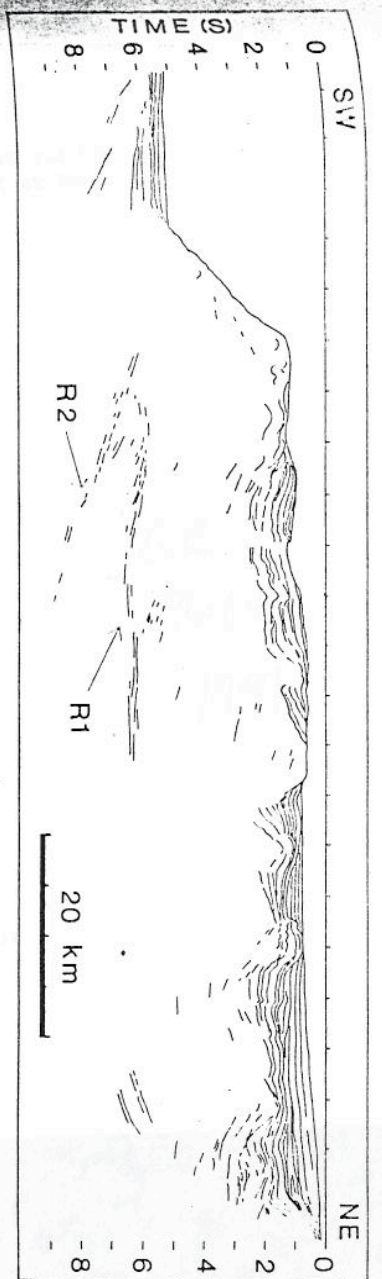


Fig. 3. Line drawing of profile RU-3 after poststack, finite difference, time migration. R1 and R2 are deep events related to the subducted oceanic plate (VE=4). Symbols same as in Figure 1.

Lucia and Santa Maria basins, (2) the abrupt
 upper slope break and the steep continental
 slope, (3) a largely nonreflective layer
 underlying the strata of the Neogene basins, and
 (4) two sets of high-amplitude, deep events (R1
 and R2), beginning approximately 15 km landward
 of the slope base. At the southwest end of the
 profile, the Pacific plate is shown intersecting
 the continental slope. The oceanic crust of the
 Pacific plate is overlain by a 0.5-1.0 s thick
 reflection sequence and dips landward between 5.5
 and 6.5 s two-way travel time. The steep (10°-
 18°) continental slope is a rough surface,
 perhaps due to small slump deposits, underlain by
 the nonreflective layer. Similar slope morphology
 continues northwest approximately 35 km (Figure
 1) to the intersection with the fossil transform
 at Lonsdale (1991). The Santa Lucia Basin
 lies landward of the upper continental slope.

This basin is bounded on its seaward edge by
 light folds and thrust faults and on its landward
 edge by the Santa Lucia Bank. RU-3 exhibits a
 slightly thicker stratigraphic section than the
 0.75-s thickness commonly observed on seismic
 reflection data across other parts of the basin
 (McCulloch, 1987). To the northeast of the basin
 Lucia Basin, on the Santa Lucia Bank, upper
 Cretaceous to Eocene rocks are exposed on the
 seafloor (Hosgrl and Griffiths, 1971). These
 units return few coherent reflections and were
 referred to as acoustic basement by Page et al.
 (1979).

The offshore Santa Maria Basin lies landward
 of the Santa Lucia Bank and extends to the
 northeast end of RU-3. In this basin, the
 basement structure is observed in RU-3 and
 northeast-southwest to form an en echelon pattern
 related to compressional tectonic faulting
 (McCulloch, 1987).

the continental margin exhibits only scattered
 reflections. These events probably result from
 isolated blocks of bedded rock or faults within
 the presumed accretionary complex. Below this
 poorly reflective layer, two sets of high-
 amplitude events are visible on the seaward
 portion of RU-3. As discussed below, these
 events, designated R1 and R2 in Figure 3, are
 associated with subducted oceanic lithosphere.
 Other deep events occur within the basement of
 the Pacific plate on the seaward end of RU-3 and
 at 5.0-7.0 s below the offshore Santa Maria
 Basin.

Depth Conversion

A simplified depth section (Figure 4) shows
 the correct spatial relationships among the
 geologic features. Velocities for depth
 conversion were derived from analyses of
 reflected arrivals in the reflection data that
 are evident in reversed shot-receiver gather
 pairs. These analyses provided velocities for
 the upper (1-2 km) sedimentary section in the
 Santa Maria Basin, for the deformed rocks east of
 the Hosgrl fault, and for the rocks below the
 Santa Lucia Bank. Based on these analyses, rock
 velocities within the offshore Santa Maria Basin
 increase from 1.6 km/s just below the seafloor to
 4.1 km/s at approximately 2.5-3.0 s two-way
 travel time. In contrast, the deformed rocks
 east of the Hosgrl fault have a compressional
 velocity of approximately 4.0 km/s near the
 seafloor. In parts of the basin with relatively
 dipping strata, interval velocities derived from
 stacking velocity analysis compared well with the
 reflection-derived velocities.
 A two-layer velocity model was used for depth

JGR
 96(4)
 1991

F6-87-NC

Sample #	Type	Comments
Fe Mn CRUSTS		
D8-2	BULK (0-24) Type 1	CC, XRD
D8-7A	BULK CRUST (0-20) T3	CC, XRD, REE
D8-4A	CRUST LAYER (0-16) T2 Porous-Mn cemented SS; L 1	CC, XRD
D8-4B	CRUST LAYER (16-27) T2 massive, dense; laminated- wavy L 2&3	CC, XRD
D8-4C	CRUST LAYER (27-45) T2 massive, dense; massive, porous L 4&5	CC, XRD
D8-6A	CRUST LAYER (0-5) T3 laminated	CC, PGE, AU, REE, XRD
D8-6B	CRUST LAYER (5-13) T3 laminated	CC, PGE, AU, REE, XRD
D8-6C	CRUST LAYER (13-20) T3 laminated--most dense	CC, PGE, AU, REE, XRD
D8-8C	BULK CRUST (0-23) T3+4	CC, REE, XRD
D8-8C	CRUST LAYER (0-6) T3+4	XRD
D8-8C	CRUST LAYER (6-16) T3+4	XRD
D8-8C	CRUST LAYER (16-23) T3+4	XRD
D8-9F	BULK CRUST T4	CC, REE, XRD
SUBSTRATE		
D8-2B	MUDSTONE (MN FREE)	OC, XRD
D8-9A	MUDSTONE	OC, REE, XRD
D8-9B	BOXWORK BLADES	OC, REE, XRD
D8-9C	LT BROWN CLAY INFILLING BOXWORK	XRD
D8-9D	WAXY COHERENT SEDIMENT NEARER TO BOXWORK	XRD
D8-9E	SEDIMENT FURTHER AWAY FROM BOXWORK	XRD
D8-6D	Mn dendritic mudstone	OC, XRD
D8-7B	Mn free mudstone	OC, XRD
D8-8A	YELLOW BOXWORK	XRD
D8-8B	CREAM BOXWORK	XRD
D8-8B-1 (D8-8B(2))	BULK BOXWORK	OC, REE, XRD
D8-8D	MUDSTONE	OC, REE, XRD
D8-9	BOXWORK BLADES	XRD

T1 = Large nucleus surrounded by Mn

T2 = Mn nodules, small nucleus

T3 = crust

T4 = crust underlain by boxwork

D8-7(1) Mudstone matrix
7(2) Siltstone clastD8-8(1) Pink clay A
w/ BoxworkD8-8(2) Light colored
pocket in A

D8-8B(1) Black faxes

D8-8B(2) Bulk boxwork

D8-8D(1) Siltstone

D8-9(1) MS 'in' boxwork